Concurrent Optimization of Signal Progression and Crossover Spacing for Diverging Diamond Interchanges

Yao Cheng[1]; Gang-Len Chang, M.ASCE[2]; and Saed Rahwanji[3]

Abstract: Diverging diamond interchanges (DDIs) are widely recognized to be capable of reducing conflict points, number of stops, and consequently average traffic delay. However, the design of their crossover spacing and signal offsets, which is critical to the capacity and efficient operations of DDIs, have not been addressed in most design guidelines. These two critical design components are actually interdependent in nature, because the estimated travel time between a DDI's two subintersections for all movement paths is essential for the design of signal offsets. Also, the crossover spacing should be designed to accommodate queues comprised mostly of those vehicles not moving within the signal progression band, which is often designed with a given crossover spacing. Considering such an interdependent relation between signal offsets and the crossover spacing, this study presents a model that can concurrently optimize these two vital DDI design elements at the planning level. A case study at a DDI site with the proposed model has also been conducted to justify the necessity to perform the concurrent optimization under different operational conditions. The results of extensive numerical experiments confirm that the design with the optimized crossover spacing and offset can yield the shortest total delay and the least number of stops for vehicles over the entire network, especially under near-saturated conditions. The optimized crossover spacing can also prevent the formation of the queue spillover over the crossovers in a DDI. **DOI: 10.1061/JTEPBS.0000121.** © *2018 American Society of Civil Engineers.*

Author keywords: Crossover spacing; Signal offsets; Concurrent optimization.

Introduction

As one of the most widely applied unconventional intersection/interchange designs, diverging diamond interchanges (DDIs) have been extensively discussed by the traffic community (Chilukuri et al. 2011; Edara et al. 2005; Rasband et al. 2012; Maji et al. 2013; Hu et al. 2014; Tian et al. 2015). Compared to a conventional diamond interchange, a DDI can reduce conflict points for the turning movements from and onto freeway ramps by reversing the through movements at the crossovers, as shown in Fig. 1. By crossing the through movements in opposing directions, the number of signal phases has been reduced to two, which results in less lost time and better use of the signal timings.

In the 2000s, Chlewicki (2003) investigated the DDI concept and employed a simulation for its performance comparison before and after implementation. Siromaskul and Speth (2008) tested the traffic performance of conventional diamond interchanges, single-point urban interchanges (SPUIs), and DDIs with *VISSIM* under five different demand patterns. The results show that SPUIs outperform conventional diamond interchanges in most cases, but prove less effective than DDIs. For all cases, DDIs yield less delay than conventional diamond interchanges, especially for high off-ramp left-turn volumes. Bared et al. (2005) used *VISSIM* to analyze double crossover interchanges (DXIs) and DDIs with different numbers of lanes under various demand patterns. The existence of pedestrian volumes was also considered in the analysis. Their study concluded that both DXIs and DDIs, compared to the conventional design, result in lower (60%) total delay under high-volume cases and comparable performance at the lower demand level. They further indicated that DDIs nearly double the capacity for left-turn movements under the conventional diamond design. This study also concluded that DDIs are more financially efficient than widening the bridge of a conventional diamond interchange under higher traffic volume conditions. Similar conclusions have also been made by Hughes et al. (2010), from their research of comparing the performance of DDIs of four or six lanes with a conventional diamond design in terms of throughput, delay, number of stops, queue length, safety impacts, and construction costs. Chlewicki (2011) further evaluated the performance of the aforementioned three designs and pointed out that SPUIs outperform a conventional diamond interchange in most cases but yield more delays than DDIs. Their study also found that the efficiency of a DDI, when compared with other designs, increases with the number of lanes.

The advantages of DDIs further extend to the safety aspects because of the reduction in conflict points and signal phases. For example, Claros et al. (2015) conducted a safety evaluation of six DDI sites in Missouri using three types of before-and-after evaluation methods: naive, empirical Bayes, and comparison group. They found that the DDI can trade high-severity crashes for low-severity crashes since the reduction in fatal and injury crashes (FI) is more significant than for property damage crashes (PDO). Using the data of seven sites from four states, Hummer et al. (2016) concluded that a DDI to replace a diamond interchange should reduce all crashes by 33%. Angle and turning crashes were found to decrease more significantly than rear-end crashes. Claros et al. (2016) developed the crash modification factors (CMFs) for DDI ramp terminals for different crash severity levels using the data from

[1]Ph.D. Candidate, Dept. of Civil and Environmental Engineering, Univ. of Maryland, 3111 Kim Engineering Bldg., College Park, MD 20742 (corresponding author). ORCID: https://orcid.org/0000-0002-0513-0272. E-mail: chengyao09@gmail.com

[2]Professor, Dept. of Civil and Environmental Engineering, Univ. of Maryland, 3111 Kim Engineering Bldg., College Park, MD 20742. E-mail: gang@umd.edu

[3]Assistant Division Chief, Office of Traffic and Safety, Maryland State Highway Administration, 7491 Connelley Dr., Hanover, MD 21076. E-mail: srahwanji@sha.state.md.us

Note. This manuscript was submitted on April 13, 2017; approved on September 5, 2017; published online on January 2, 2018. Discussion period open until June 2, 2018; separate discussions must be submitted for individual papers. This paper is part of the ***Journal of Transportation Engineering, Part A: Systems***, © ASCE, ISSN 2473-2907.

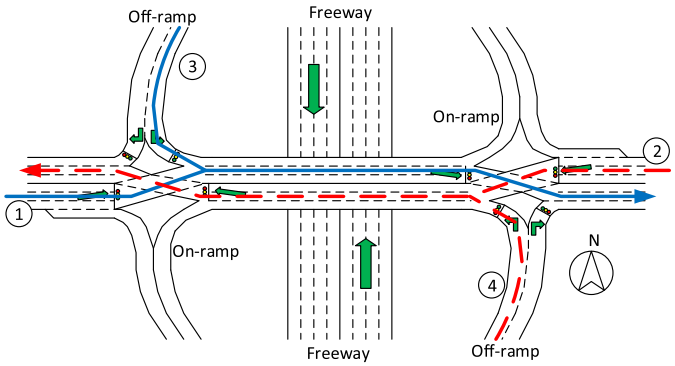

Fig. 1. Geometric design and critical movements of a DDI

20 ramp terminals. By reviewing more crash reports, Claros et al. (2017) further developed several crash prediction models for ramp terminals in DDIs.

To estimate the queue length on a DDI, Chang et al. (2011) defined four types of queues and calibrated the models with extensive simulation experiments. A delay model was also derived to account for the unique features of a DDI. From a theoretical perspective, Xu et al. (2011) developed a control delay model that can yield reliable results when comparing those from a well-calibrated simulator. Considering the progression of movements between two crossover intersections in a DDI and between neighboring adjacent intersections, Yang et al. (2014) developed a signal optimization model based on whether or not an exclusive left-turn lane was implemented. This study also considered the optimization of offsets at adjacent intersections to improve the efficiency of the whole system. Their models, under the simulation platform developed with *VISSIM*, have been shown to outperform the plan generated by Synchro under all volume cases.

However, despite the increasing attention on DDI, some fundamental issues remain to be studied. For example, the crossover spacing, most critical to the operational capacity of a DDI, has not been addressed in most operation guidelines. Since the crossover spacing of a DDI cannot be significantly adjusted after construction, it is rather important to determine its length in advance, based on the projected traffic volume. Because they are mainly designed to accommodate the traffic flows near ramps, DDIs often experience high volumes of turning traffic flows from the off-ramp during peak hours, and thus insufficient crossover spacing may cause frequent queue spillovers at their signals. For example, as shown in Fig. 1, when the westbound vehicles are not discharged effectively on the crossover, the spillover may block the eastbound through movement at the east intersection and the off-ramp flows from the northbound of the freeway. These excessive queues may also dramatically affect the lane-changing behavior of westbound vehicles on the crossover. On the other hand, a crossover spacing that is longer than needed is not desirable either, since it will yield a longer travel time and a longer ramp to connect the intersections and the freeway.

Most importantly, from the queue formation perspective, it is noticeable that the optimal crossover spacing is interdependent with the optimal progression offsets within the DDI and its volumes for all movements. Moreover, since the crossover spacing is often constrained by the geometry condition and it is hardly possible to change the spacing after construction, a proper length for the crossover spacing is critical at the planning level. Hence, concurrent optimization of signal progression and crossover spacing in a DDI best achieves its operational efficiency and also minimizes construction costs.

In view of such potential benefits, this study presents an optimization model that can concurrently yield the optimal signal offsets and crossover spacing, considering the potential queues on the crossovers and also the travel time, as well as the delay, encountered by vehicles in each movement on a DDI. The proposed model is developed for use at the planning level as a guideline for construction and preliminary traffic control.

Research Issues

This study is focused on a typical DDI with exclusive left-turn lanes to the on-ramps and traffic signals for both left-turn and right-turn flows at the off-ramps. To ensure the efficient operations of such a DDI, one needs to address the following critical issues:

- Design of the optimal cycle length and signal timing plan for each subintersection;
- Design of the optimal distance between stop lines for each movement passing two subintersections to avoid queue spillback; and
- Design of the optimal offsets to best facilitate the progression of all path flows.

The first issue can certainly be solved independently with any existing signal design method (Webster 1958; Wong and Wong 2003). Because of the design of reversed movements between the crossovers, each intersection in a DDI has only two phases. To facilitate the flexibility of the proposed model, this study adopts separate controllers at two subintersections as suggested by Hughes et al. (2010). Specifically, as shown in Fig. 2, let the first phase be defined as the one used by eastbound through and southbound right (northbound left at the east crossover) flows; the second phase is to serve the westbound through and southbound left (northbound right at the east crossover) volumes. The offset for the west intersection is set to be zero.

However, the second and third issues must be solved concurrently because the relation between the crossover spacing and the signal offset is interdependent in nature. Although DDIs have reduced conflict points, their through vehicles and left-turn vehicles from the off-ramps (see four critical movements in Fig. 1) have to pass two subintersections. Because of the short distance between these two intersections, the designed offset for those movements will determine the progression level for vehicles between those two subintersections and the resulting queues at the crossover.

More specifically, to optimize the offset, the estimated travel time between two subintersections along these movement paths must be obtained, which requires the knowledge of the crossover spacing. However, the crossover spacing should be designed to accommodate queues contributed by those vehicles that cannot benefit from the progression. Hence, determining the crossover spacing without considering the offsets at the preliminary stage of construction may result in excessive queues and less effective operations. Thus, it is essential to concurrently optimize both the crossover spacing and the signal offsets to best the capacity and efficiency of a DDI.

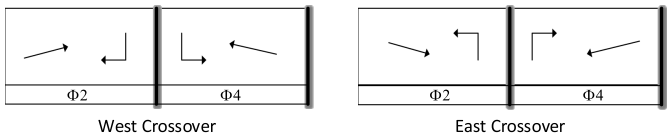

Fig. 2. Ring-and-barrier diagram for the signal setting at two crossovers of a DDI

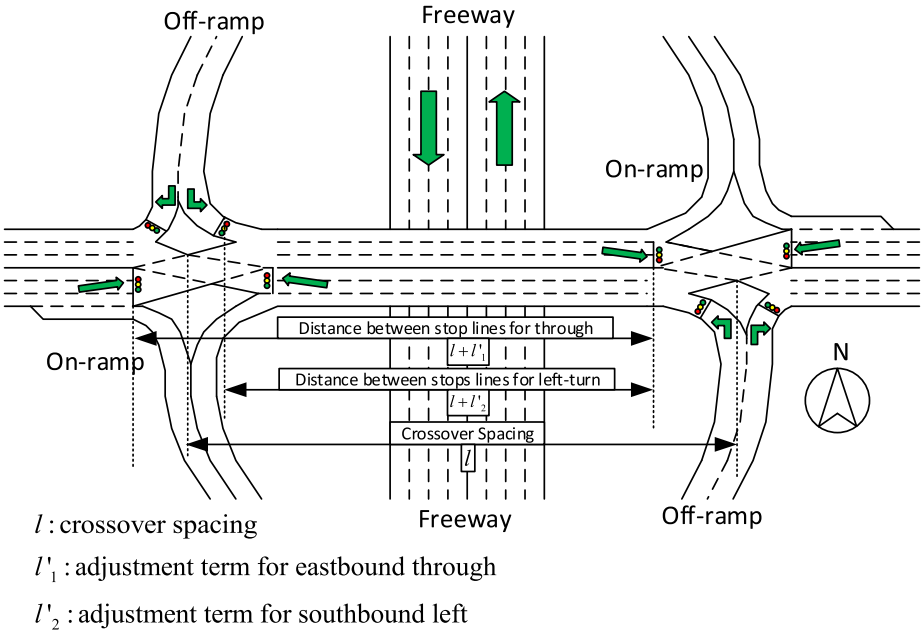

Fig. 3. Crossover spacing and distances between stop lines on a DDI

As shown in Fig. 3, the distances between the stop lines along the through and left turn paths over the crossover are significantly different. That is due to the unique features of DDIs, which contain two off-ramps in opposing directions. Hence, a set of adjustment terms should be set on the crossover spacing to reflect the differences between the crossover spacing and the distance between the stop lines. Such adjustment terms depend on whether it is for off-ramp left turn or through movements. The distances in Fig. 3 are measured along the vehicle paths.

In brief, given the cycle length and signal timings at each subintersection, one can concurrently optimize the crossover spacing and signal offsets. The model formulations for such an optimization are presented below.

Offset and Crossover Spacing Optimization

In this section, the formulations to optimize progressions and crossover spacing will be introduced, respectively, followed by a discussion of the necessity to combine these two designs into one model.

Offset Optimization

Among existing methods in the literature for maximizing the progression band, *MAXBAND* (Little et al. 1981) remains the one offering the best efficiency. As such, this study adopts the core logic of *MAXBAND* as the basis for the design of signal progression.

Taking the DDI in Fig. 1 as an example, those four movements, which pass the two subintersections, are defined as critical movements, and their performances are significantly affected by the signal offsets. For convenience of presentation hereafter, they are numbered as (1) eastbound through; (2) westbound through; (3) southbound left; and (4) northbound left. Fig. 4 shows the notations used in the formulations, and the progression bands for all critical movements in a DDI. To facilitate the discussion, the west intersection shown in Fig. 4 is denoted as Intersection 1 and the east one as Intersection 2.

The following objective function shown in Eq. (1) is proposed to maximize the total bandwidth for all movements in a DDI:

$$\text{Max:} \sum_j b_j \tag{1}$$

where b_j = progression bandwidth for critical movement j, in fraction of a cycle, as shown in Fig. 4. To optimize the offset for the DDI, one sets proper constraints to ensure the existence of such bands. The first group of constraints to reflect the interference is introduced to make sure that the designated band for each movement only uses its corresponding green phase, which can be expressed as follows (Fig. 4):

$$w_{i,j} + b_j \le g_{i,j} - t_c \tag{2}$$

$$w_{i,j} \ge 0 \tag{3}$$

where $w_{i,j}$ = part of green time before the specified band used by flows on movement j at intersection i, in fraction of a cycle; $g_{i,j}$ = duration of the phase for movement j at intersection i, including the clearance time, in fraction of a cycle; and t_c = clearance time (all-red time) at the end of each phase, in fraction of a cycle. Because of the distance between stop bars of through movements

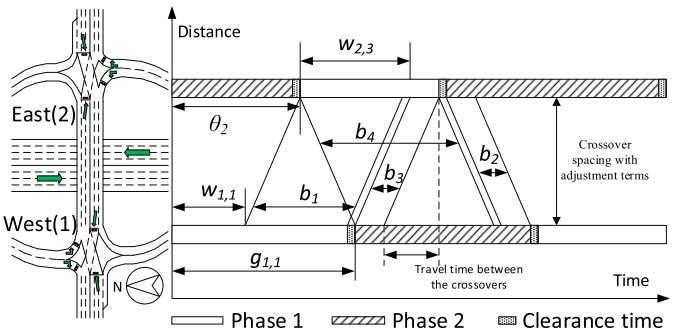

Critical paths: 1: eastbound through 2: westbound through
3: southbound left 4: northbound left

Fig. 4. Progression bands on a DDI

at a DDI crossover, clearance time between green phases should not be ignored.

Then, a group of progression constraints should be specified to determine the proper offsets that are able to produce the bands for all path flows. Taking Path 1 as an example, this set of constraints can be introduced as follows:

$$\theta_1 + w_{1,1} + \frac{l + l_1'}{v_1 C} + n_{1,1} = \theta_2 + w_{2,1} + n_{2,1} \tag{4}$$

where θ_i = offset at intersection i, in fraction of a cycle; l = variable for crossover spacing, in meter; C = predetermined cycle length, in seconds; l_i' = distance adjustment term based on the crossover spacing defined by the position of the stop lines for movement i, in meter; v_j = progression speed defined for critical movement j, in m/s; and $n_{i,j}$ = integer variables which represents number of cycles. The third term on the left-hand side of Eq. (4) denotes the travel time between stop lines for movements on Path 1 calculated with an average speed, as shown in Fig. 4. The left-hand side of Eq. (4) denotes the distance between the start of the eastbound through band and the vertical axis at Intersection 1 plus the corresponding travel time, and the right-hand side denotes the similar distance at Intersection 2. Forcing these two terms to be equal would ensure the existence of the progression band. At this stage, the crossover spacing and adjustment term are assumed to be predetermined as in the state of most practices.

Likewise, one can follow the same notion to derive the progression constraints for the other three critical paths as follows:

$$\text{Movement 2: } \theta_2 + g_2 + w_{2,2} + \frac{l + l_2'}{v_2 C} + n_{2,2} = \theta_1 + g_1 + w_{1,2} + n_{1,2} \tag{5}$$

$$\text{Movement 3: } \theta_1 + g_1 + w_{1,3} + \frac{l + l_3'}{v_3 C} + n_{1,3} = \theta_2 + w_{2,3} + n_{2,3} \tag{6}$$

$$\text{Movement 4: } \theta_2 + w_{2,4} + \frac{l + l_4'}{v_4 C} + n_{2,4} = \theta_1 + g_1 + w_{1,4} + n_{1,4} \tag{7}$$

where g_i = duration of Phase 1 at intersection i, including the clearance time, in fraction of a cycle.

Given the crossover spacing and an estimated travel time between the stop lines for each movement, one can then formulate the offset optimization model with Eqs. (1)–(7). Notably, different lengths for the crossover spacing may lead to different maximum bandwidths and optimized offsets.

Crossover Spacing Optimization

To avoid unnecessarily long ramps and excessive construction cost, the crossover spacing should be minimized under the geometric constraints. Therefore, the objective of the crossover spacing optimization model can be expressed as

$$\text{Min: } l \tag{8}$$

Although a shorter crossover spacing is preferred in terms of construction cost and operation benefits, it should be sufficiently long to avoid queue spillover. Fig. 5 illustrates the logic to compute the queue length based on the traffic flows, which can be expressed as follows:

$$\tau = \frac{(Cr + \delta)\alpha q \cdot s}{s - \alpha q} \tag{9}$$

where τ = distance between the stop bar and the end of queue before it is fully discharged, in numbers of vehicles; r = fraction of red phase; δ = lost time in seconds; q = volume, in vph; α = corresponding lane use factor denoting the ratio of actual traffic volume on the heaviest-used lane over that on the whole lane group (i.e., 0.55 for two lanes and 0.4 for three lanes in this study); and s = saturation flow rate. In Eq. (9), $(Cr + \delta)\alpha q$ represents the number of queueing vehicles at the end of a red phase. As long as the queue can be fully discharged during the green phase, the most distant point to which the queue can be extended in a cycle can be obtained by multiplying that queue length with $s/(s - \alpha q)$, which is the ratio between the saturation flow and queue accumulation rates.

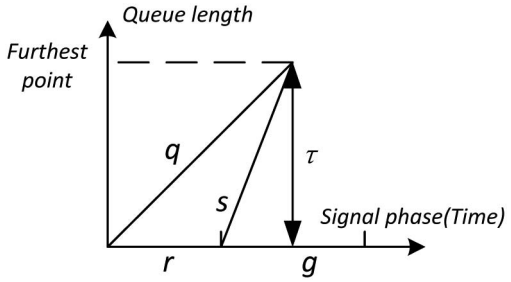

Fig. 5. Queue length estimation

Eq. (9) is derived with the assumption of uniform arrivals. However, because of the short distance between the two subintersections, the resulting queue length at the end of a red phase would be highly dependent on the offsets and both the off-ramp and the through-movement flows between those subintersections.

Taking the eastbound movement between two subintersections as an example (Fig. 3), the traffic queues at the end of a red phase consist of most off-ramp and through vehicles that cannot experience progression. The queue consisting of those vehicles can be expressed by the traffic volume multiplied with an uncoordinated fraction of green time, which is $\alpha q_1(g_1 - b_1 - t_c)C/(g_1 - t_c)$ and $\alpha q_3(1 - g_1 - b_3 - t_c)C/(1 - g_1 - t_c)$, respectively, for through and off-ramp vehicles. The queue length depends on the heaviest-used lane between the crossovers, so a lane-use factor is adopted in the formulation, and it may be affected by the geometry condition at the DDI site, such as lane configurations at the crossovers. The most distant point to which the queue length is extended can then be derived in the same manner as for Eq. (9), considering that the incoming flows may consist of vehicles from either of those two movements. This most distant point should not exceed the crossover spacing.

Therefore, to ensure that the minimal length for the distance between subintersections is sufficient to accommodate those two streams of flows, one needs to further specify the following constraints:

$$\begin{aligned} &\frac{s}{s - \alpha q_j}[\alpha q_1(g_1 - b_1 - t_c)C/(g_1 - t_c) \\ &\quad + \alpha q_3(1 - g_1 - b_3 - t_c)C/(1 - g_1 - t_c)] \\ &\quad \le (l + l_3')/h, \quad j = 1, 3 \end{aligned} \tag{10}$$

where h = spatial headway of vehicles between two subintersections, in meter. $(g_1 - b_1 - t_c)/(g_1 - t_c)$ represents the portion of uncoordinated eastbound through vehicles, and $(1 - g_1 - b_3 - t_c)/(1 - g_1 - t_c)$ is for the off-ramp vehicles, assuming the uniform distribution of arrivals during the green phase at the west intersection. The two terms in the bracket denote the numbers of vehicles not within the progression bands from the eastbound through and southbound off-ramp left-turn movements, respectively. The sum is then multiplied by the first term in Eq. (10) to obtain the maximum queue length in a cycle, based on the movements contributing

to the queue formation after the east subintersection ends its red phase. Eq. (10) should be satisfied regardless of whether the incoming flows are from through or off-ramp turning movement. The right-hand side of Eq. (10) denotes the maximum number of queueing vehicles that can be stored on each lane between the two subintersections.

Likewise, the constraint for the queues at the west intersection, which accounts for both westbound through and northbound off-ramp left turn, is specified as follows:

$$\frac{s}{s-\alpha q_j}[\alpha q_2(1-g_2-b_2-t_c)C/(g_2-t_c) + \alpha q_4(g_2-b_4-t_c)C/(g_2-t_c)] \le (l+l_4')/h, \quad j=2,4 \tag{11}$$

These two constraints assume that all vehicles not within the progression band will form the queues. Eqs. (10) and (11) are specified to avoid queue spillback regardless of the signal phase at the upstream intersection when the downstream intersection ends its red phase. At this stage, the optimization model for the crossover spacing is based on the given bandwidths, which can be directly computed from the offset.

The following constraints are then introduced to specify the reasonable ranges for the crossover spacing, and the adjustment terms for the distance between stop lines:

$$l_{\min} \le l \le l_{\max} \tag{12}$$

$$l_{t,\min} \le l_1', l_2' \le l_{t,\max} \tag{13}$$

$$l_{l,\min} \le l_3', l_4' \le l_{l,\max} \tag{14}$$

where l_{min} (l_{max}) = lower (upper) bounds for the crossover spacing, in meter; $l_{t,min}$ ($l_{t,max}$) and $l_{l,min}$ ($l_{l,max}$) are used for the adjustment terms for through movement and off-ramp left-turn flows, indicating the difference between the crossover spacing and the distance between stop lines for different movements. The range for the crossover spacing should be determined by the width of the freeway mainline, available right-of-way, and other geometry conditions. The ranges for each adjustment term are determined by the size of the median island at the intersection for the off-ramp (Fig. 3) and the number of lanes in each approach at the subintersections.

Given the computed offsets and the resulting bandwidths for each movement, one can formulate the optimization model for the crossover spacing with Eqs. (8), (10)–(14). Different offsets may lead to different optimal crossover spacings, because the size of the uncoordinated flows, contributing directly to the queue vehicles, varies with the level of progression.

Concurrent Optimization of Offset and Crossover Spacing

In brief, it is noticeable that the crossover spacing plays a key role in the design of the optimal offset. The progression bandwidth, computed with the offsets, in turn affects the potential queue size and the required crossover spacing. Such an interdependent relation can also be viewed in Fig. 4, where changing the crossover spacing will inevitably vary the travel time between intersections, and consequently the bandwidths for those movements.

Eq. (15) presents a new objective function that integrates Eq. (1) with Eq. (8) to reflect the necessity of concurrently optimizing the crossover spacing and the signal offsets. Considering that minimizing crossover spacing should be of less importance than the smooth traffic operations, a weighting factor is introduced to make sure that the total bandwidth can dominate the crossover spacing in the optimization process

$$\text{Max:} \sum_j b_j - \frac{l/vC}{M} \tag{15}$$

where v = predetermined vehicle average speed between the ramp terminals, in fps, and M is a large number serving as a weighting factor. M should be sufficiently large (i.e., 10,000 in this study) such that the crossover spacing is dominated by the optimal value of the bandwidths. The second term in Eq. (15) represents the estimated travel time between two subintersections in fraction of a cycle. With a rather large value of M, the solution procedures to maximize the objective function will first guarantee the optimal offset and then identify the proper crossover spacing.

All required constraints for the integrated objective function are listed in Eqs. (2)–(7) and (10)–(14). Unlike those independently optimized models, the concurrent optimization model views neither the offset nor the crossover spacing as a known parameter. Thus, the travel time between these two subintersections is viewed as a variable, varying with the actual distance between the stops lines for each critical movement (Fig. 3) and the progression speed of traffic flows. The potential vehicle queues between these subintersections will then depend on the resulting offsets. By doing so, the optimization results shall yield the best offset and the optimal crossover spacing.

In summary, the proposed model for concurrently optimizing the crossover spacing and signal progression consists of the following objective function and constraints:

$$\text{Max:} \sum_j b_j - \frac{l/v}{C \times M}$$

Subject to Eqs. (2)–(7)

Eqs. (10)–(14)

$0 \le b_j, \quad \theta_i \le 1, \quad n_{i,j}$: integers

The objective function and all constraints are linear and the proposed model can be solved with linear programming solver packages. This study shows a model to be applied to a DDI where all off-ramp movements and through movements at the crossovers are signalized and exclusive left-turn lanes exist for on-ramps. The formulations can be applied to other cases with case-specific modification. For example, as shown in Fig. 1, if the southbound left-turn movement is not signalized but subject to a yield sign, progression constraints for this movement should be removed and Eq. (10) should consider that the through movement and the left-turn movement concurrently contribute to the queue length after the red phase at the east crossover ends.

Case Study

Test Site

To evaluate the potential of the proposed optimization model, this study has selected a DDI at I-70 and Mid Rivers Mall Drive in Saint Peters, Missouri, for experimental analysis. As shown in Fig. 6, the actual crossover spacing is 143 m (469 ft). The p.m. peak demand data from a traffic survey in April 2016 are presented in Table 1. The demand volumes for movement paths passing two subintersections are also shown in Fig. 6, where these paths are also denoted with arrows. The lane configuration and green splits, calculated with the Webster method (Webster 1958), are also listed in Table 2. All those off-ramp movements are controlled by the signal

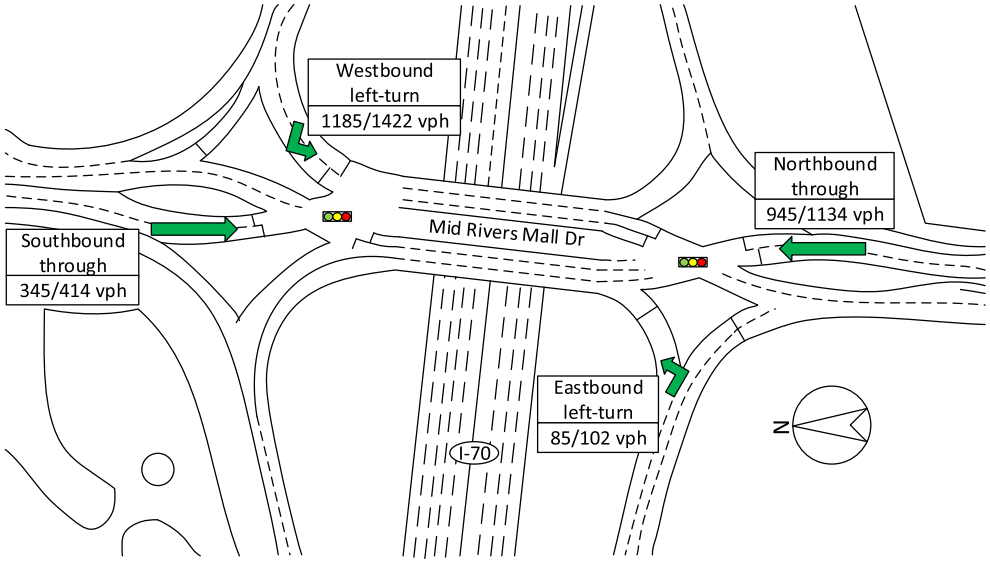

Fig. 6. DDI at I-70 and Mid Rivers Mall Drive in Saint Peters, Missouri

at each subintersection. The phase duration in the table includes 3 s of yellow time and 4 s of all-red duration.

Some other key parameters used in the case study are listed below.

- The progression speed: 56 km/h (35 mph).
- The yellow time: 3 s per phase.
- The all-red clearance time: 4 s per phase.
- The saturation flow rate: 1,600 vph.
- The cycle length: 115 s.
- The lower bound and upper bound for the crossover spacing: 122 m (400 ft) and 305 m (1,000 ft), respectively.
- The lower and upper bounds for these adjustment terms for through movements: −3 m (−10 ft) and 3 m (10 ft); for off-ramp left-turn: −34 m (−110 ft) and −18 m (−60 ft).
- The lane use factor: 0.55 for two lanes, and 0.4 for three lanes.
- The spatial headway of the vehicles in the queue between subintersections: 8 m (25 ft).

Table 1. Volume Distribution at the Test Site

Direction	Left (vph)	Through (vph)	Right (vph)
Southbound	120	345	490
Northbound	150	945	595
Eastbound	85	—	635
Westbound	1,185[a]	—	150

[a]Off-ramp movements with highest volume.

Table 2. Lane Configuration and Signal Information at the Test Site

	North intersection		South intersection	
Movement	Number of lanes	Phase time (s)	Number of lanes	Phase time (s)
Southbound through	2	32	2	63
Northbound through	2	83	2	52
Off-ramp left turn	2	83	1	63
Off-ramp right turn	2	32	2	52

Optimization Results and Simulation Design

To verify the effectiveness of the proposed model, the authors of this research have conducted a case study under two demand patterns and different crossover spacings with simulation. Using the signal information calculated with the volumes shown in Table 1, the proposed model is solved by *CPLEX* ILOG on a desktop with an Intel i7 processor and 16 GB RAM. It yields the optimized crossover spacing of 203 m (667 ft), with the through and left-turn adjustment factors of 3 m (10 ft) and −34 m (−110 ft), respectively, for both directions.

To validate the necessity of concurrent optimization, this study has further applied the proposed model with two predetermined crossover spacings other than the actual crossover spacing for simulation analysis. The shorter crossover spacing of 173 m (568 ft) is selected from the average of the actual and the optimized lengths, while the longer one is set with the upper limit of crossover spacing in mind. The offsets for these three cases for comparison are then calculated with the proposed model, using the crossover spacing as a parameter instead of a variable. However, since the queues between the crossovers cannot be constrained if the length of the crossover is not sufficient, Eqs. (10) and (11) were removed from the proposed model in computing their optimal offsets.

To test the proposed model's effectiveness under congested conditions, a high-volume scenario, 1.2 times the current volume, has also been adopted to evaluate the performance of the proposed model under congested and near-saturation traffic conditions. Using the same signal split information, the proposed model yields the crossover spacing of 245 m (803 ft), for the high-demand scenario. The crossover is larger in order to facilitate the longer potential queue caused by higher volume. The performance of different DDI crossover spacings under such high-demand conditions has also been evaluated in the experimental analysis. The selected crossover spacings for comparison as well as their offsets between two subintersections in the DDI are shown in Table 3.

To evaluate the performance of the proposed model, this study has further used PTV *VISSIM*, a traffic simulation tool, to simulate those cases listed in Table 3. The measurements of effectiveness for network performance evaluation include the average delay per

Table 3. Cases for Simulation Analyses

Cases	Current volume		Projected volume (1.2 times)	
	Crossover spacing (m)	Offset (s)	Crossover spacing (m)	Offset (s)
1. Actual	143	24	143	24
2. Shorter	173	40	173	40
3. Optimized	203	42	245	44
4. Long	274	46	274	46

vehicle, average number of stops per vehicle, and the average vehicle speed in the network. The average delays for vehicles on all critical movements have also been included in the evaluation. Time-dependent queue lengths between the crossovers at two subintersections are also discussed.

Simulation Results

Figs. 7 and 8 show the resulting measurements of effectiveness from five simulation replications of 2 h for the current and projected volumes.

Figs. 7 and 8 show that the optimized crossover spacing outperforms the other three cases with respect to all three measures of effectiveness (MOEs), especially for the case with the projected volumes. The average delay per vehicle decreases from Case 1 to Case 3, reflecting that increasing the length for the crossover spacing toward the optimal one can result in less traffic delay. However, the improvement cannot be substantiated with the excessively long length for the crossover spacing as shown in Case 4 of 274 m (900 ft), which indicates that a longer length of crossover is not always beneficial if it is beyond the optimal value.

Table 4 further shows the average delay of all the critical paths passing two subintersections under the current and projected volumes. Westbound left-turn flows, the highest volume of 1,185 vph, can experience the lowest delay with the optimized design under the projected volume. The advantage of the optimized crossover spacing and the offsets is more significant under high-volume conditions. Under the current volume, although the optimized design does not yield the lowest delay for westbound through movement, it never causes significantly high delay for any movement compared to other designs and it is still able to yield average delay for all movements, as shown in Fig. 7.

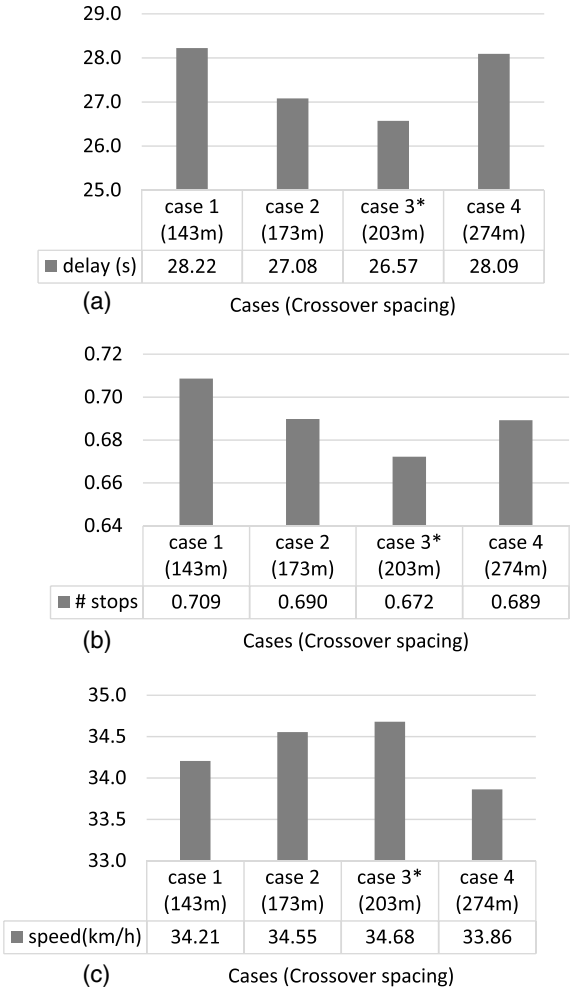

Fig. 7. MOEs for the current volume under different crossover spacings and progression designs: (a) average delay per vehicle (s); (b) average number of stops per vehicle; (c) average speed of vehicles in the network (km/h)

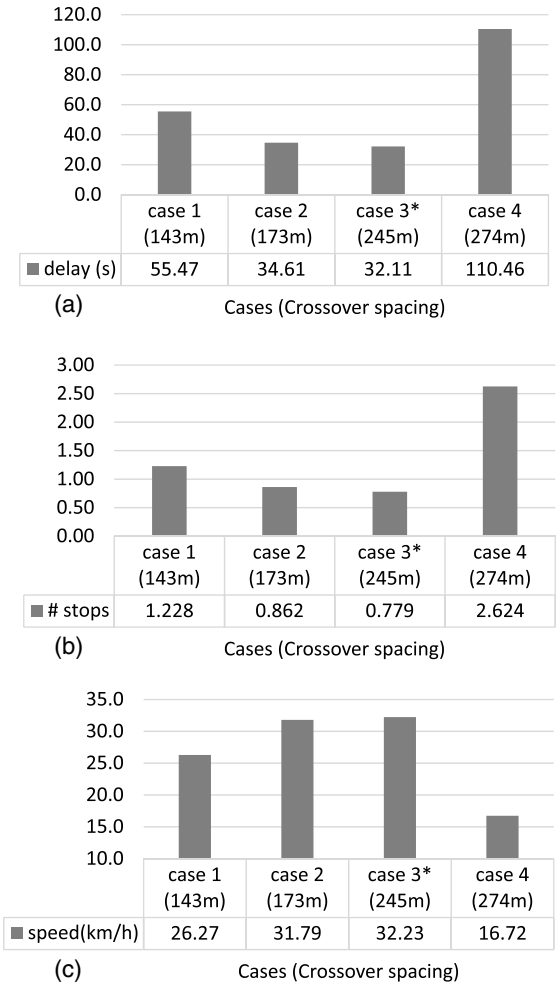

Fig. 8. MOEs for the projected volume under different crossover spacings and progression designs: (a) average delay per vehicle (s); (b) average number of stops per vehicle; (c) average speed of vehicles in the network (km/h)

Table 4. Average Delay of All Critical Paths under Two Volume Scenarios

Volume scenarios	Cases (crossover spacing)	Southbound through (s)	Northbound through (s)	Westbound left turn (s)	Eastbound left turn (s)
Current volume	1. (143 m)	66.6	53.3	28.1	18.8
	2. (173 m)	73.9	49.1	30.0	18.1
	3. (203 m)[a]	73.5	46.0	31.0	17.1
	4. (274 m)	120.0	38.4	98.7	19.8
Projected volume (1.2 times)	1. (143 m)	151.9	62.8	44.9	19.1
	2. (173 m)	80.0	54.8	42.3	14.4
	3. (245 m)[a]	71.4	31.6	28.8	16.0
	4. (274 m)	111.2	38.4	77.8	17.3

[a]The optimal design.

The time-dependent queue lengths between the subintersections in Cases 1 and 3 under the current volume are shown in Fig. 9, where the dashed lines show the spacing between two stop lines for left turning vehicles to demonstrate when the queue may spill over. By comparing the results in Figs. 9(a and b), one may find that the queues between the crossovers at the south intersection may spill back occasionally in Case 1 (the existing design). Yet, the optimized crossover spacing is able to accommodate the variation in traffic demand. In Case 1, the queues may sometime spill back at the north intersection, but it will not occur under the case with the optimized crossover spacing. This result demonstrates the critical role of the optimized crossover spacing along with signal progression in preventing the formation of traffic blockage in a DDI design.

The key findings from the case study are listed below:

- The concurrently optimized crossover spacing and signal plan can indeed produce the lowest average vehicle delays and least number of stops compared with those cases that design these two key components sequentially.
- The design of a DDI with the proposed optimization model can better accommodate the surge and fluctuation in traffic volume from all movements.
- A crossover spacing longer than the optimized one may result in excessive travel times for some movements and consequently reduce the operational capacity of a DDI.
- The optimized crossover spacing, coupled with the optimized offsets, can prevent the formation of queue spillback in a

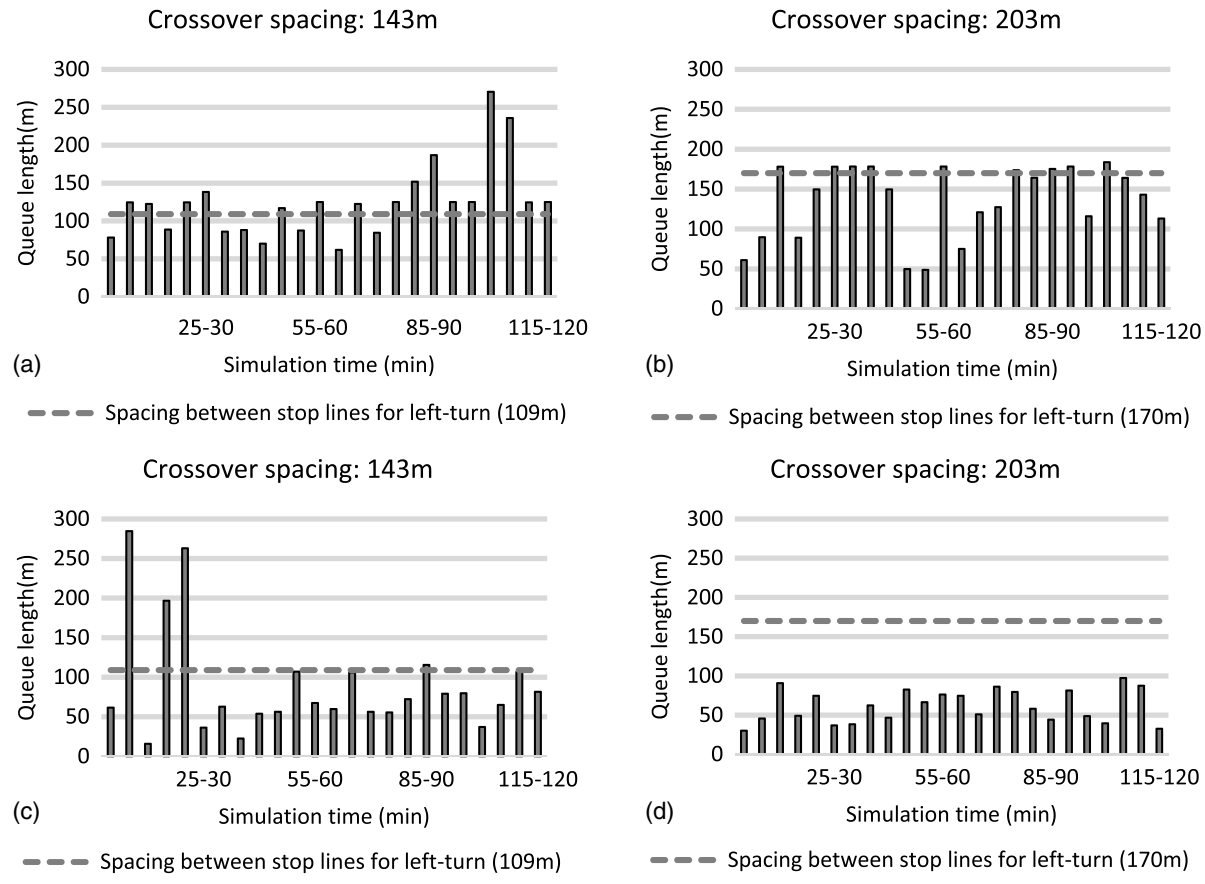

Fig. 9. Time-dependent queue lengths between the crossovers: (a) time-dependent queue length at the south intersection in Case 1; (b) time-dependent queue length at the south intersection in Case 3; (c) time-dependent queue length at the north intersection in Case 1; (d) time-dependent queue length at the north intersection in Case 3

DDI. Any design for a DDI with insufficient length for the crossover spacing often results in frequent traffic blockages.
- The benefits of the concurrently optimized crossover spacing and offsets increase with the volume to be accommodated by the DDI.

Conclusions

This study has developed a model to concurrently optimize the crossover spacing and the signal offsets in a DDI, based on the cycle length and green split. The proposed model can fully account for the interdependent relation between the crossover spacing and the signal offsets between the two subintersections in a DDI, thus ensuring that the produced crossover spacing is sufficient to avoid queue spillback. To evaluate the performance of the proposed model, this study has further used simulation to analyze traffic movements and their resulting delay with different designs of the crossover spacing. The results from simulation experiments clearly show that DDI with the concurrently optimized crossover spacing and offsets can yield the shortest delays and travel times. Moreover, the DDI with the optimized design features can effectively cope with potential queue spillback on the crossovers and the surge, as well as fluctuation in traffic volume. In brief, the proposed model has shown its promise for potential field applications, especially at the preliminary stage, to evaluate the interrelation between signal offsets and crossover spacing.

One critical topic for future research should be developing a method to concurrently optimize the cycle length and signal offsets of DDI subintersections and adjacent intersections together with the crossover spacing. Considering the adjacent intersections when optimizing the offsets at crossovers would further improve the efficiency of the system since the traffic pattern arriving at the crossovers is significantly affected by the upstream offsets. More studies along this line will include developing (1) a method to determine whether or not to set signals for all off-ramp flows at those DDI subintersections; (2) guidelines for the choice between a shared left turn or exclusive left turn to the on-ramp flows; and (3) a method to estimate the effect on adjacent freeway exits.

Acknowledgments

The authors are grateful for the kindly help from MO DOT on providing traffic volume data for the test site. This study is supported by the Maryland SHA ATTAP Program, Traffic and Safety and Operations Lab, at the University of Maryland, College Park.

References

Bared, J., Edara, P., and Jagannathan, R. (2005). "Design and operational performance of double crossover intersection and diverging diamond interchange." *Transp. Res. Rec.*, 1912, 31–38.

Chang, G. L., Lu, Y., and Yang, X. (2011). "An integrated computer system for analysis, selection, and evaluation of unconventional intersections." *Rep. No. MD-11-SP909B4H*, Maryland State Highway Administration, Baltimore.

Chilukuri, V., Siromaskul, S., Trueblood, M., and Ryan, T. (2011). "Diverging diamond interchange: Performance evaluation (I-44 and Route 13)." *Rep. No. OR11-012*, Missouri Dept. of Transportation, Jefferson City, MO.

Chlewicki, G. (2003). "New interchange and intersection designs: The synchronized split-phasing intersection and the diverging diamond interchange." *2nd Urban Street Symp.: Uptown, Downtown, or Small Town: Designing Urban Streets That Work*, Anaheim, CA, 28–30.

Chlewicki, G. (2011). "Should the diverging diamond interchange always be considered a diamond interchange form?" *Transp. Res. Rec.*, 2223, 88–95.

Claros, B., Edara, P., and Sun, C. (2016). "Site-specific safety analysis of diverging diamond interchange ramp terminals." *Transp. Res. Rec.*, 2556, 20–28.

Claros, B., Edara, P., and Sun, C. (2017). "When driving on the left side is safe: Safety of the diverging diamond interchange ramp terminals." *Accid. Anal. Prev.*, 100, 133–142.

Claros, B. R., Edara, P., Sun, C., and Brown, H. (2015). "Safety evaluation of diverging diamond interchanges in Missouri." *Transp. Res. Rec.*, 2486, 1–10.

CPLEX [Computer software]. IBM, New York.

Edara, P. K., Bared, J. G., and Jagannathan, R. (2005). "Diverging diamond interchange and double crossover intersection: Vehicle and pedestrian performance." *3rd Int. Symp. on Highway Geometric Design*, Chicago.

Hu, P., Tian, Z. Z., Xu, H., and Andalibian, R. (2014). "An advanced signal phasing scheme for diverging diamond interchanges." *93rd Annual Meeting of the Transportation Research Board*, Washington, DC.

Hughes, W., Jagannathan, R., Sengupta, D., and Hummer, J. E. (2010). "Alternative intersections/interchanges: Informational report (AIIR)." *Rep. No. FHWA-HRT-09-060*, FHWA, Washington, DC.

Hummer, J. E., et al. (2016). "Safety evaluation of seven of the earliest diverging diamond interchanges installed in the United States." *Transp. Res. Rec.*, 2583, 25–33.

Little, J., Kelson, M. D., and Gartner, N. H. (1981). "MAXBAND: A program for setting signals on arteries and triangular networks." *Transp. Res. Rec.*, 795, 40–46.

Maji, A., Mishra, S., and Jha, M. K. (2013). "Diverging diamond interchange analysis: Planning tool." *J. Transp. Eng.*, 0.1061/(ASCE)TE.1943-5436.0000603, 1201–1210.

Rasband, E., Forbush, T., and Ash, K. (2012). "UDOT diverging diamond interchange (DDI) observations and experience." *Rep. No. UT-12.05*, Utah Dept. of Transportation, Salt Lake City.

Siromaskul, S., and Speth, S. B. (2008). "A comparative analysis of diverging diamond interchange operations." *ITE 2008 Annual Meeting and Exhibit Institute of Transportation Engineers*, Washington, DC.

Tian, Z. Z., Xu, H., De Camp, G., Kyte, M., and Wang, Y. (2015). "Readily implementable signal phasing schemes for diverging diamond interchanges." *94th Annual Meeting of the Transportation Research Board*, Washington, DC.

VISSIM [Computer software]. PTV AG, Karlsruhe, Germany.

Webster, F. V. (1958). *Traffic signal settings*, Vol. 39, HMSO, London.

Wong, C. K., and Wong, S. C. (2003). "Lane-based optimization of signal timings for isolated junctions." *Transp. Res. Part B: Methodol.*, 37(1), 63–84.

Xu, H., Liu, H., Tian, Z. Z., and Zhang, W. (2011). "Control delay calculation at diverging diamond interchanges." *Transp. Res. Rec.*, 2257, 121–130.

Yang, X., Chang, G. L., and Rahwanji, S. (2014). "Development of a signal optimization model for diverging diamond interchange." *J. Transp. Eng.*, 10.1061/(ASCE)TE.1943-5436.0000657, 04014010.